Talanta 233 (2021) 122578

Contents lists available at ScienceDirect

Talanta

journal homepage: www.elsevier.com/locate/talanta

A neoteric dual-signal colorimetric fluorescent probe for detecting endogenous/exogenous hydrogen peroxide in cells and monitoring drug-induced hepatotoxicity

Lanlan Xu [a], Yu Zhang [c], Lihe Zhao [a], Hao Han [a], Siqi Zhang [a], Yibing Huang [c], Xinghua Wang [a], Daqian Song [a], Pinyi Ma [a,**], Ping Ren [b,***], Ying Sun [a,*]

[a] College of Chemistry, Jilin Province Research Center for Engineering and Technology of Spectral Analytical Instruments, Jilin University, Qianjin Street 2699, Changchun, 130012, China
[b] Department of Thoracic Surgery, The First Hospital of Jilin University, Xinmin Street 71, Changchun, 130021, China
[c] College of Life Sciences, Jilin University, Qianjin Street 2699, Changchun, 130012, China

ARTICLE INFO

Keywords:
Fluorescent probe
Hydrogen peroxide
Cell imaging
Colorimetric detection
Drug-induced liver injury

ABSTRACT

Hydrogen peroxide (H_2O_2), one of the most important reactive oxygen species (ROS), can be generated endogenously in the liver and has been deemed as a biomarker for evaluating drug-induced liver injury (DILI). Therefore, it is highly crucial to construct an effective method for detecting H_2O_2 in the liver in order to evaluate DILI. Herein, a neoteric dual-signal colorimetric fluorescent probe XH-2 for sensing hydrogen peroxide was engineered and synthesized. Borate was grafted as a specific recognition group onto the fluorophore XH-1 (Φ_F = 0.34) to establish a structurally unprecedented probe. The experimental results manifested that probe XH-2 (Φ_F = 0.15) was able to detect hydrogen peroxide using a fluorescence method with an excellent linear range of 0–140 μM (R^2 = 0.9974) and an especially low detection limit of 91 nM ($\lambda_{ex/em}$ = 570 nm/638 nm). In addition, the probe was capable of monitoring hydrogen peroxide in a colorimetric manner with the linear range of 0–110 μM (R^2 = 0.9965). Furthermore, the specificity, applicability in serum (98.6–109.1%) and indirect detection of glucose make the probe XH-2 a superior probe. Based on its low cytotoxicity, the probe was successfully applied to monitor endogenous/exogenous hydrogen peroxide and quantitatively determine the concentration level of hydrogen peroxide at a range of 0–120 μM (R^2 = 0.9859) in HepG2 cells. Ultimately, the probe could effectively monitor the level of hydrogen peroxide during DILI in HepG2 cells.

1. Introduction

Reactive oxygen species is a single electron reduction product of oxygen produced in the human body [1] that has a significant impact on many physiological processes [2] and pathological processes. As one of the most important reactive oxygen species, hydrogen peroxide plays a vital role in physiological processes such as cell migration, proliferation [3], differentiation and immunity [4]. However, abnormal levels of hydrogen peroxide in the cell can damage nucleic acids, proteins [5], and biofilms, and can cause many diseases [6], such as Alzheimer's disease, Parkinson's disease, cardiovascular disease, and cancer [7], diabetes, neurodegenerative diseases [8,9], etc. Therefore, it is important to develop a highly sensitive and selective method for the rapid and effective detection of intracellular hydrogen peroxide concentration.

Thus far, various analytical methods for detecting hydrogen peroxide have been developed, which can include fluorescence spectroscopy [10–25], spectrophotometry, electrochemistry [26], titration method, positron emission tomography [27], chemluminescence [28], electron spin resonance [29], and mass spectrometry [30]. Among all, the fluorescence spectroscopy has increasingly become the method of choice because of its noninvasiveness, high sensitivity, high selectivity, low cost, simple operation, and high spatiotemporal resolution, and its target analytes can be monitored and imaged in living cells [31–34].

* Corresponding author.
** Corresponding author.
*** Corresponding author.
E-mail addresses: mapinyi@jlu.edu.cn (P. Ma), rpemail@jlu.edu.cn (P. Ren), yingsun@jlu.edu.cn (Y. Sun).

https://doi.org/10.1016/j.talanta.2021.122578
Received 4 March 2021; Received in revised form 26 May 2021; Accepted 27 May 2021
Available online 1 June 2021

Additionally, long-wavelength emission fluorescent probes are preferred because long-wavelength photons have deeper tissue penetration and less interference from auto-fluorescence [35]. To further rule out influences of other interferences, such as detection conditions and human errors, NIR fluorescent probes with multiple response signals can be used, especially in the biomedical fields, so that the detection results are more convincing and trustable. Therefore, it is very important to develop colorimetric and fluorescent dual-signal NIR probe for the detection of hydrogen peroxide.

Herein, a neoteric dual-signal colorimetric fluorescent probe XH-2 for detecting hydrogen peroxide was designed and synthesized. Compound XH-1 was designed to function as a fluorophore and borate a recognition group. In the absence of hydrogen peroxide, probe XH-2 exhibited infinitesimal fluorescence because of the photoinduced electron transfer (PET) activated by $\lambda_{ex/em}$ = 570 nm/638 nm. In the presence of hydrogen peroxide, the chemical reaction between hydrogen peroxide and the borate recognition group of probe XH-2 eventually caused the borate part to separate, while caused probe XH-2 to be converted into compound XH-1. These events led to the enhancement of fluorescence, accompanying by the color change from bright yellow to bright red under a 365 nm fluorescent lamp or from yellow to red under visible light when observed with the naked eye. Probe XH-2 was also successfully applied to indirectly detect glucose, which was a proof of its universality. Based on its long emission wavelength, high selectivity and sensitivity, and low cytotoxicity, probe XH-2 was subsequently successfully applied to detect endogenous/exogenous hydrogen peroxide and to quantitatively detect hydrogen peroxide in HepG2 cells, as well as in the monitoring the hydrogen peroxide level in drug-induced liver cells.

2. Experimental section

2.1. Synthesis

The synthetic route of probe XH-2 is shown in Scheme 1.

2.1.1. Synthesis of compound 1

The synthesis of compound 1 was carried out according to the previously published method [36].

2.1.2. Synthesis of compound XH-1

At room temperature, compound 1 (0.153 g, 1.1 mmol) and 1-naphthol (0.144 g, 1 mmol) were mixed with 5 mL of CH_2Cl_2 in a reaction bottle, and the mixture was then stirred evenly. After that, 3 mL of hydrochloric acid was added dropwise to the reaction bottle for 5 h. The product was purified by silica gel chromatography using a mixture of petroleum ether and ethyl acetate (v/v = 5:1) as the mobile phase, from which compound XH-1 as an dark red solid (130 mg, 65%) was afforded. ^{1}H NMR (300 MHz, DMSO-d_6) δ 8.60 (d, J = 8.0 Hz, 1H), 8.14 (d, J = 7.8 Hz, 1H), 7.85 (t, J = 7.5 Hz, 1H), 7.78 (d, J = 7.4 Hz, 1H), 7.70 (d, J = 8.7 Hz, 1H), 6.85 (d, J = 8.8 Hz, 1H), 6.76 (s, 1H), 6.36 (s, 1H) (Fig. S4). ^{13}C NMR (75 MHz, DMSO-d_6) δ 182.42, 161.50, 151.35, 145.32, 142.41, 132.03, 131.33, 131.20, 131.09, 131.01, 126.14, 125.11, 123.82, 114.02, 105.70, 105.64, 101.77 (Fig. S5). MS (LC-HRMS, m/z) for $C_{16}H_{10}NO_3^+$ $[M+H]^+$: calculated, 264.0655; found: 264.0658 (Fig. S1).

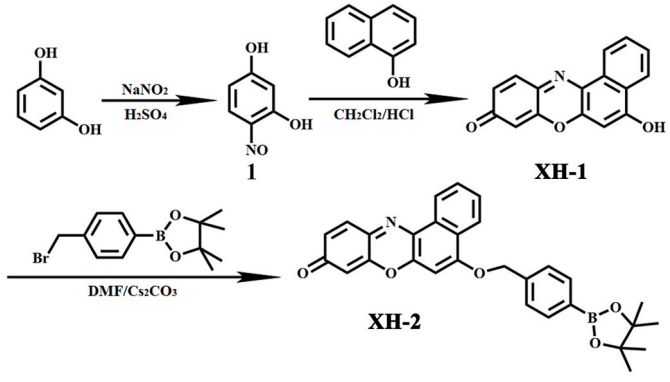

Scheme 1. The synthetic route of probe XH-2.

2.1.3. Synthesis of probe XH-2

At room temperature, compound XH-1 (0.263 g, 1 mmol), 4-bromomethylphenylboronic acid pinacol ester (0.594 g, 2 mmol) and Cs_2CO_3 (0.651 g, 2 mmol) were mixed with 5 mL of DMF in a reaction bottle, and the mixture was stirred evenly for 6 h. The product was purified by silica gel chromatography using a mixture of petroleum ether and ethyl acetate (v/v = 10:1) as the mobile phase, and probe XH-2 as lightly yellow solid (283 mg, 59%) was obtained. ^{1}H NMR (300 MHz, $CDCl_3$) δ 8.71–8.66 (m, 1H), 8.32–8.28 (m, 1H), 7.86 (d, J = 8.1 Hz, 2H), 7.80–7.70 (m, 3H), 7.45 (d, J = 8.2 Hz, 2H), 6.99 (dd, J = 8.8, 2.7 Hz, 1H), 6.87 (d, J = 2.6 Hz, 1H), 6.43 (s, 1H), 5.20 (s, 2H), 1.35 (s, 12H) (Fig. S6). ^{13}C NMR (75 MHz, $CDCl_3$) δ 183.74, 161.33, 151.19, 145.31, 144.25, 138.69, 135.16, 131.89, 131.74, 131.38, 131.11, 130.81, 127.58, 126.47, 125.74, 124.26, 113.44, 106.88, 101.11, 83.88, 70.52, 24.83 (Fig. S7). MS (LC-HRMS, m/z) for $C_{29}H_{27}BNO_5^+$ $[M+H]^+$: calculated, 480.1977; found: 480.1980 (Fig. S2).

2.2. Studies of absorption and fluorescence properties

The reactions in PBS solution (10 mM, pH = 7.4) were monitored using an UV–Vis spectrophotometer and F-7000 fluorescence spectrometer. Both the probe XH-2 and compound XH-1 have excellent water solubility. When observed with the naked eye in PBS (10 mM, pH = 7.4), they appeared light yellow and light red respectively. The fluorescence intensity increased 7.0 times in detecting hydrogen peroxide. The fluorescence measurements from 590 nm to 750 nm were conducted at an excitation wavelength of 570 nm with a slit set of 5.0/5.0 nm. Prior to the measurement, the probe XH-2 (10 μM) in PBS solution was treated with various concentrations of H_2O_2 for 40 min. The selectivity of the probe XH-2 toward H_2O_2 was determined by comparing the results from H_2O_2 with those from other possible competing species under the same experimental conditions.

2.3. Preparation of solutions used in spiked recovery experiment

Firstly, human serum was 200-fold diluted, then a mixture of probe XH-2 (10 μM) with 40, 80, or 100 μM H_2O_2 separately was prepared and used for fluorescence experiment.

2.4. Indirect detection of glucose

Glucose oxidase solution (20 μg/mL) and glucose solution (0–140 μM) were incubated in PBS (pH = 8) at 37 °C for 30 min; Subsequently, probe XH-2 (10 μM) was added and the incubation was continued for 40 min.

3. Results and discussion

3.1. Optical characterizations of probe XH-2

In the fluorescence spectrum shown in Fig. 1(A), with the excitation wavelength at 570 nm, a weak emission band centered at 638 nm was observed in the absence of H_2O_2 (Φ_F = 0.15), and upon the addition of H_2O_2, the intensity of the band significantly enhanced (Φ_F = 0.34). As can be seen, under the radiation of 365 nm fluorescent lamp, the color of the solution changed tremendously from bright yellow to bright red.

In the UV–Vis absorption spectrum shown in Fig. 1(B), probe XH-2 exhibited a main absorption band centered at 455 nm ($\varepsilon = 2.8 \times 10^4$

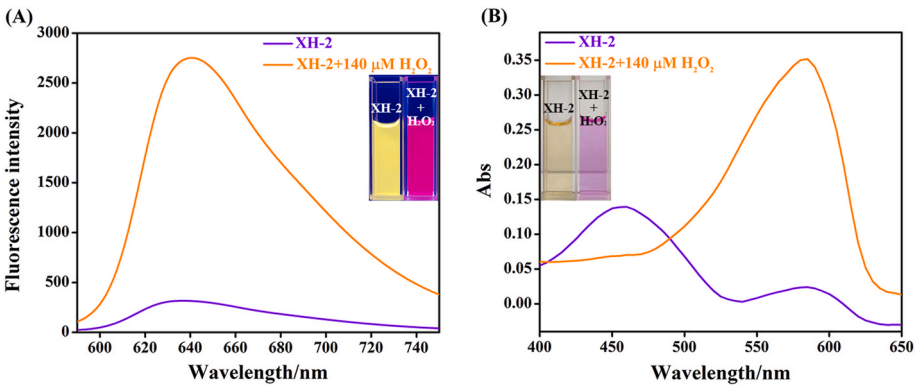

Fig. 1. (A)/(B) Fluorescence spectra/absorption spectra of probe XH-2 in PBS in the absence and presence of H_2O_2.

M^{-1} cm^{-1}) in the absence of H_2O_2, and the solution was visibly yellow. By contrast, the addition of H_2O_2 resulted in a newly generated absorption band centered at 585 nm ($\varepsilon = 4.9 \times 10^4$ M^{-1} cm^{-1}), and the color of the solution changed completely from yellow to red.

3.2. Quantitative detection of H_2O_2 by probe XH-2

In the fluorescence spectrum (Fig. 2(A)), probe XH-2 was used to detect different concentrations of H_2O_2 (0–140 μM). It was found that the fluorescence intensity of the peak centered at 638 nm increased with increasing concentration of H_2O_2. As shown in Fig. 2(B), the concentration of H_2O_2 in a range of 0–140 μM had a linear relationship (R^2 = 0.9974) with the fluorescence intensity, indicating that the probe XH-2 could quantitatively detect H_2O_2. The detection limit was determined, using the formula DL = 3σ/k, to be as low as 91 nM, which indicates that the probe XH-2 could accurately detect H_2O_2. According to Table S1, the detection limit of probe XH-2 was lower than that of most previously reported fluorescent probes. Under irradiation by a 365 nm fluorescent lamp, the solution color gradually changed from bright yellow to bright red.

In the UV–Vis absorption spectrum, as depicted in Fig. 2(C), the intensity of the absorption band centered at 455 nm gradually decreased with increasing concentration of H_2O_2, while that of the absorption band centered at 585 nm increased. As presented in Fig. 2(D), the concentration of H_2O_2 at a range of 0–110 μM had a linear relationship (R^2 = 0.9965) with the absorbance at 585 nm, indicating that probe XH-2 can quantitatively detect H_2O_2 in a colorimetric manner, as well as by the transition of color from yellow to red, which can be observed by the naked eye.

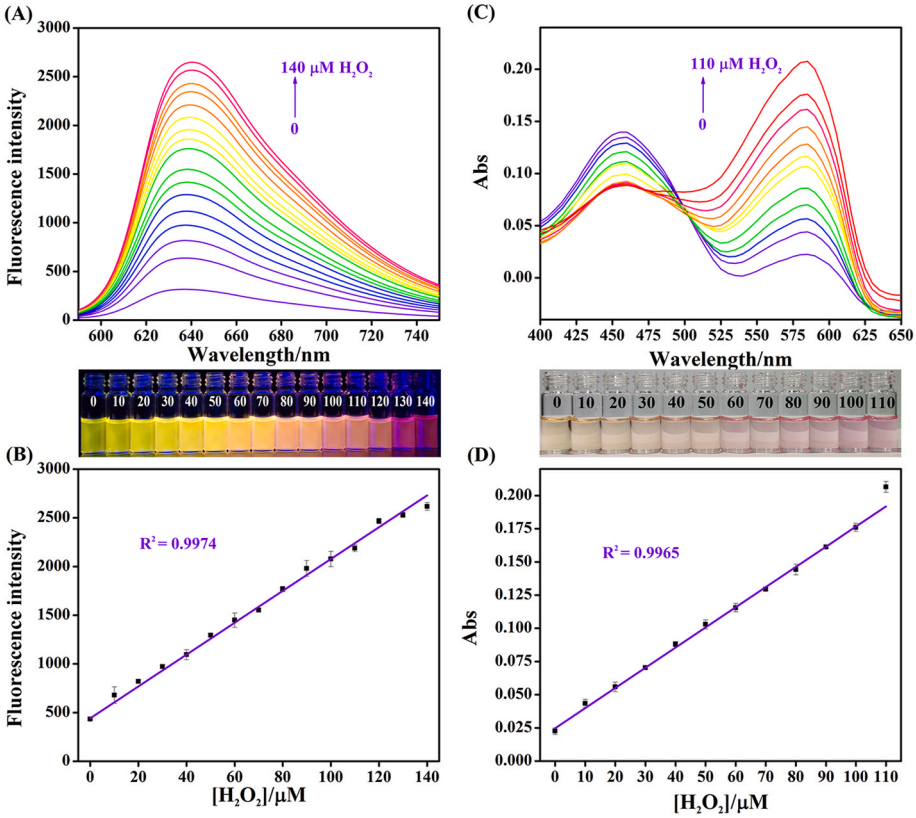

Fig. 2. (A) Fluorescence spectra of probe XH-2 (10 μM) in the presence of H_2O_2 (0–140 μM). (B) Variation of fluorescence intensities of probe XH-2 as a function of H_2O_2 concentrations (0–140 μM). (C) Absorption spectra of probe XH-2 (10 μM) in the presence of H_2O_2 (0–110 μM). (D) Variation of absorbance of XH-2 as a function of H_2O_2 concentrations (0–110 μM).

3.3. Optimizing the detection conditions

The stability is an important property of probe, and the high stability of probe is beneficial to the accuracy of the detection results. Firstly we evaluated the stability of XH-2, as shown in Fig. S8, the results indicated that XH-2 had a relatively good stability.

The effect of pH on the detection of H_2O_2 by probe XH-2 was studied. As shown in Fig. S9(A), neutral pH to alkaline pH was more beneficial to the detection of H_2O_2. Considering the physiological pH of the living system, pH = 7.4 was selected as the optimum pH and used in subsequent experiments.

Since the response time is an important parameter that can be used to evaluate the performance of reaction-based fluorescent probes, the kinetics of the reaction of XH-2 with H_2O_2 was studied by fluorescence spectroscopy (Fig. S9(B)). As the reaction time progressed, the fluorescence intensity gradually increased and became stabilized at 40 min; Thus, we used 40 min as the test time in subsequent experiments.

3.4. Selectivity of probe XH-2 toward H_2O_2

In order to evaluate the specificity of the probe XH-2 toward H_2O_2, potential interfering substances including cations, anions, reactive oxygen species and small molecules were added to the probe XH-2 solution (10 μM), and the results were compared with those when H_2O_2 (200 μM) was added. The results were shown in the Fig. 3. Unlike H_2O_2, all these potential interfering substances had no effects on the response of the probe XH-2, which indicated that the probe XH-2 had excellent specificity toward H_2O_2, guaranteeing that the probe XH-2 is suitable for use in complex living systems.

3.5. Sensing mechanism and theoretical calculations

To determine the mechanism of probe XH-2 in sensing H_2O_2, we first analyzed the fluorescence spectrum and UV–Vis absorption spectrum. As presented in Fig. 4, in both the fluorescence spectrum and the UV–Vis absorption spectrum, the peak intensity, peak shape, and peak position of probe XH-2 (10 μM) with 200 μM H_2O_2 were almost the same as those of compound XH-1 (10 μM), and the sensing mechanism may be in the direction that we expected (Scheme 2). To further prove our assumption, mass spectrometry was also employed (Fig. S1- S3). As shown in Fig. S1 and Fig. S3, the *m/z* of the mixture containing 10 μM probe XH-2 and 200 μM H_2O_2 under the test conditions for 40 min was consistent with compound XH-1, indicating that the mechanism of probe XH-2 in sensing H_2O_2 was consistent with our assumption.

We carried out theoretical calculations to understand and explain the H_2O_2-recognition mechanism of probe XH-2. The geometries of the ground and excited states and the electron structures of probe XH-2 and compound XH-1 were optimized by DFT and TDDFT calculations at the B3LYP(GD3BJ)/def2-SVP level. The result is outlined in Fig. 5. The HOMO (−6.69 eV) of the recognition unit (methylphenylboronic acid pinacol ester) was found located between the HOMO (−7.46 eV) and LUMO (−1.43 eV) of the excited-state probe XH-2, indicating that the fluorescence of probe XH-2 could be quenched by methylphenylboronic acid pinacol ester fragments as a result of intramolecular PET process. The TDDFT calculations also revealed that the maximum adsorption peak of compound XH-1 was 547.9 nm (f = 0.8051), the strong fluorescence emission peak was 625.7 nm (f = 1.1193), and the data obtained from the theoretical calculations closely resembled the experimental data. These TDDFT calculations revealed the theoretical optical properties of probe XH-2 and compound XH-1.

3.6. Detection of H_2O_2 in human serum

To further evaluate the practicability of the probe XH-2, we performed the spiked recovery test by spiking H_2O_2 into serum (200-fold dilution). The concentration of H_2O_2 in the serum sample was measured by the fluorescence method mentioned above. The results (Table 1) indicated that the probe XH-2 could successfully detect H_2O_2 in human serum samples.

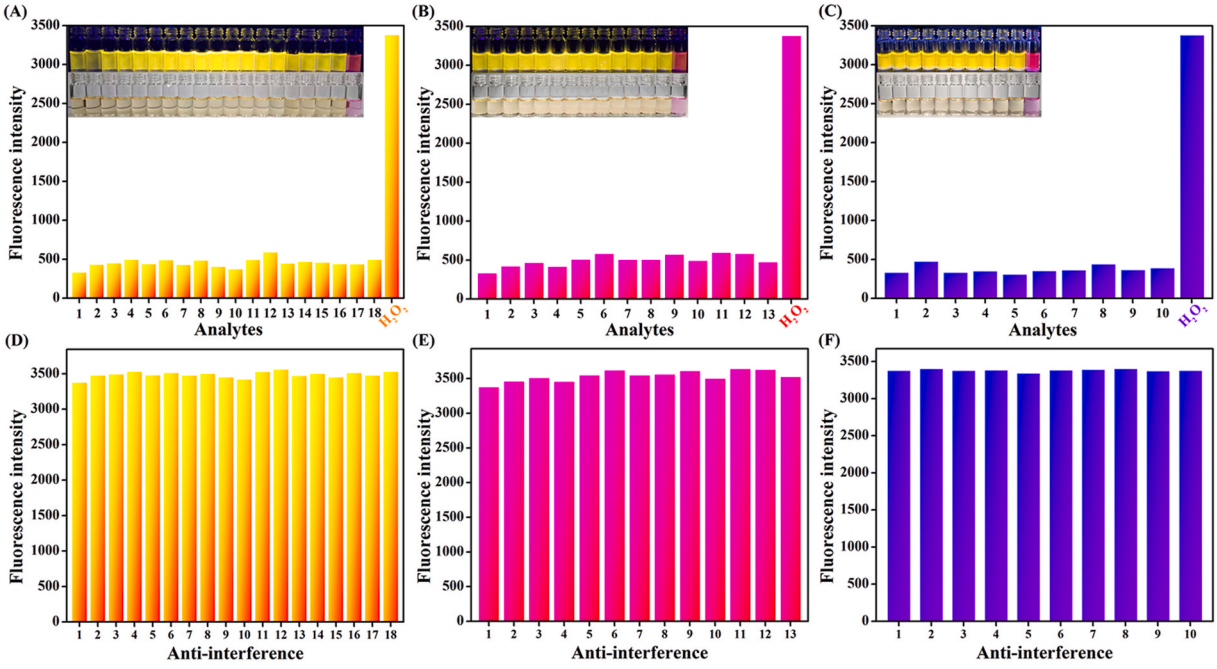

Fig. 3. (A) The fluorescence intensity of XH-2 (10 μM) to cations (1 mM) in PBS: 1. blank; 2. K^+; 3. Na^+; 4. Mg^{2+}; 5. Ca^{2+}; 6. Ag^+; 7. Pb^{2+}; 8. Li^+; 9. Zn^{2+}; 10. Cu^{2+}; 11. Ba^{2+}; 12. Fe^{3+}; 13. Ni^{2+};14. Mn^{2+}; 15. Cd^{2+}; 16. Co^{2+}; 17. Hg^{2+}; 18. Al^{3+}. (B) The fluorescence intensity of XH-2 (10 μM) to anions (1 mM) in PBS: 1. blank; 2. $H_2PO_4^-$; 3. HPO_4^{2-}; 4. HSO_4^-; 5. SO_4^{2-}; 6. CN^-; 7. F^-; 8. Cl^-; 9. Br^-; 10. I^-; 11. SCN^-; 12. AcO^-; 13. ClO_4^-. (C) The fluorescence intensity of XH-2 (10 μM) to ROS and small molecules (0.5 mM) in PBS: 1. blank; 2. TBHP; 3. TBO·; 4. NO·; 5. $\cdot O_2^-$; 6. ClO^-; 7. ·OH; 8. GSH; 9. Cys; 10. acetaminophen (APAP). (D), (E) and (F) represent respectively the fluorescence intensity of XH-2 (10 μM) in the presence of possible interference species together with H_2O_2 corresponding to (A), (B) and (C).

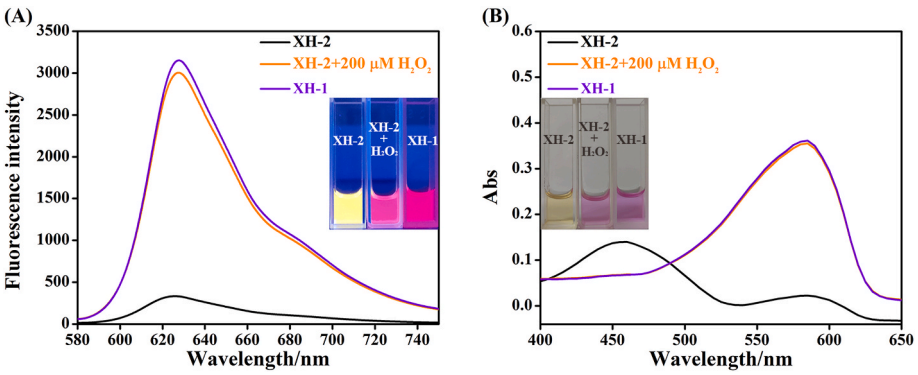

Fig. 4. (A)/(B) Fluorescence/Absorbance spectra of probe XH-2 (10 μM), probe XH-2 (10 μM) with 200 μM H_2O_2, and XH-1 (10 μM).

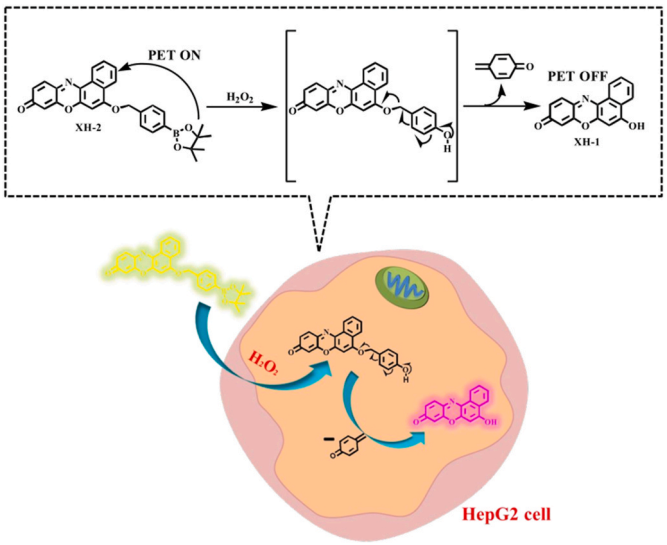

Scheme 2. The assumed H_2O_2-sensing mechanism of probe XH-2.

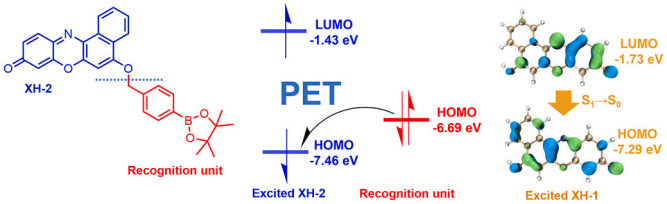

Fig. 5. HOMO/LUMO energy levels of probe XH-2 and compound XH-1 calculated based on their optimized structures of the ground and first excited states at the TDDFT levels.

Table 1
Results on recovery of H_2O_2 spiked into human serum (n = 3).

Sample	Spiked (μM)	Recovered (μM)	Recovery (%)
1	40	40.56 ± 0.37	101.4
2	80	87.33 ± 1.39	109.1
3	100	98.66 ± 1.22	98.6

3.7. Application of indirect detection of glucose

It is known that glucose can be broken down to produce the same amount of hydrogen peroxide after interacting with glucose oxidase. To further explore the versatility of probe XH-2 in biological fields, in terms of its sensitivity and specificity, probe XH-2 was applied to detect an H_2O_2-related analyte, glucose. After glucose was enzymatically oxidized by glucose oxidase, probe XH-2 could satisfactorily response to the mixture. As presented in Fig. 6(A), with increasing concentration of glucose, the intensity of the fluorescence peak centered at 638 nm gradually increased. As depicted in Fig. 6(B), probe XH-2 could indirectly detect glucose with excellent linearity (R^2 = 0.9930) at glucose concentration range of 0–140 μM. These results proved the eminent performance of probe XH-2 in indirect detection of glucose.

3.8. Fluorescence imaging of exogenous and endogenous H_2O_2 in HepG2 cells

Before performing cell imaging, we first evaluated the cytotoxicity of the probe XH-2 to HepG2 cells. The results depicted in Fig. S10 confirmed that the probe XH-2 had negligible toxicity to HepG2 cells. With the probe XH-2 at a concentration of up to 100 μM, the cell survival rate remained as high as 80%, which is a prerequisite for applying the probe XH-2 in cell imaging.

Subsequently, probe XH-2 was applied to detect exogenous/endogenous H_2O_2 in HepG2 cells. As exhibited in Fig. 7(A) and (B), the control group did not exhibit fluorescence, while HepG2 cells displayed weak fluorescence when treated with only the probe XH-2. The third group exhibited weaker fluorescence than the second group when successively treated with NAC (N-Acetyl-cysteine, an efficient antioxidant which can eliminate H_2O_2 or inhibit its production in cells) and probe XH-2. The last group, which was successively treated with NAC, H_2O_2 and probe XH-2, exhibited intense fluorescence. Thus, we drew the conclusion that probe XH-2 can be applied to monitor exogenous/endogenous H_2O_2 in HepG2 cells.

3.9. Quantitative detection of H_2O_2 in HepG2 cells

Hereafter, probe XH-2 was employed to detect different concentrations in HepG2 cells. As demonstrated in Fig. 7(C) and (D), the fluorescence of HepG2 cells became more intense as the concentration of H_2O_2 increased. A good linear relationship between fluorescence intensity and H_2O_2 concentration in a range of 0–120 μM (R^2 = 0.9859) was also observed, which demonstrates that probe XH-2 can be used for quantitative detection of H_2O_2 in HepG2 cells.

3.10. Evaluating drug-induced hepatotoxicity in HepG2 cells

Acetaminophen (APAP) is a common medicine for treating pain and fever. Excessive amounts of APAP can induce liver toxicity due to its ability to induce the production of large amounts of ROS. Therefore, with the aid of probe XH-2, the liver damage induced by APAP was evaluated using HepG2 cells and confocal imaging. As shown in Fig. 8, the fluorescence intensity of cells had an upward trend as the

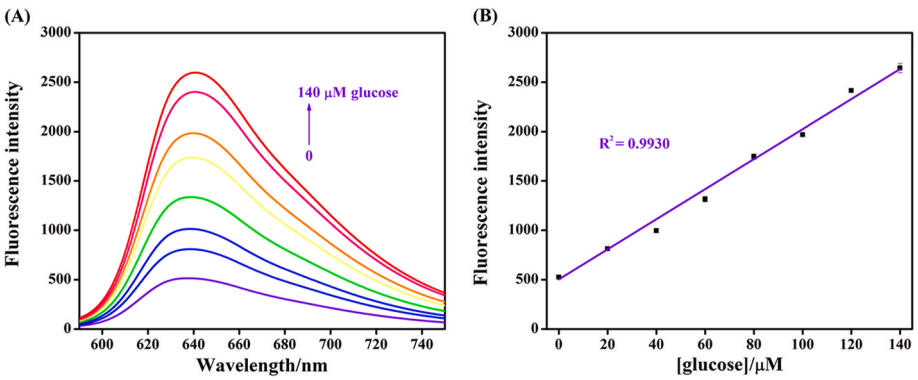

Fig. 6. (A) Change of fluorescence spectrum of probe XH-2 (10 μM) in the presence of different concentrations of glucose (0–140 μM). (B) Change of fluorescence intensity of probe XH-2 as a function of glucose concentrations (0–140 μM), $\lambda_{ex}/\lambda_{em}$ = 570 nm/638 nm.

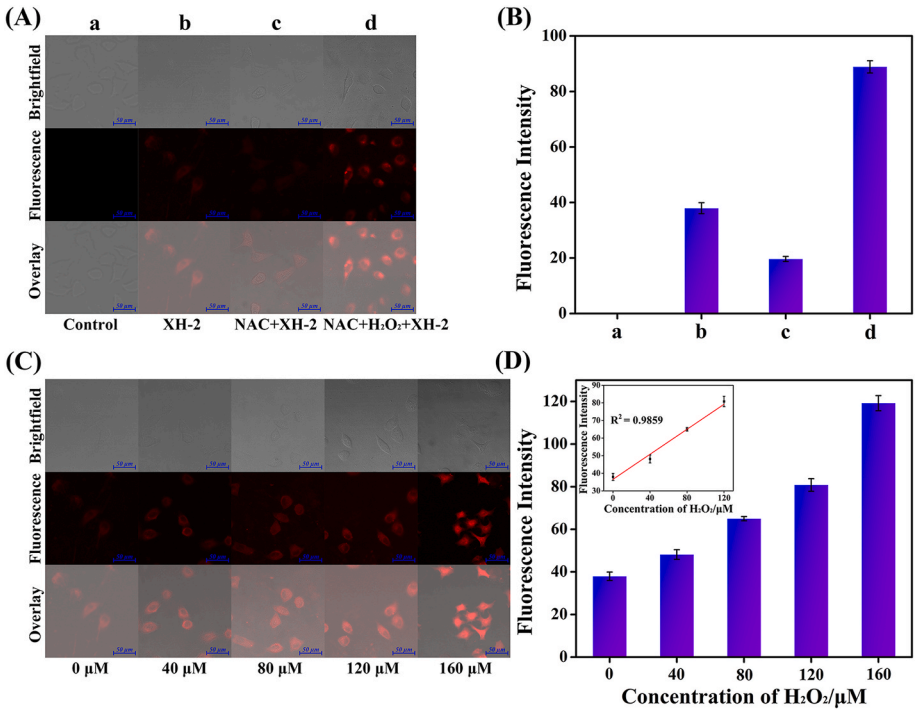

Fig. 7. (A) Fluorescence imaging of exogenous/endogenous H_2O_2 in HepG2 cells: a, control group; b, cells treated with probe XH-2 (10 μM) only; c, cells successively treated with NAC (1 mM) and probe XH-2 (10 μM); d, cells successively treated with NAC (1 mM), H_2O_2 (140 μM) and probe XH-2 (10 μM). (B) Bar graphs representing the fluorescence intensities of a, b, c, and d in (A). (C) Fluorescence imaging in HepG2 cells during the quantitative detection of H_2O_2 at different concentrations (0–160 μM). (D) Bar graphs representing the corresponding fluorescence intensities of samples in (C).

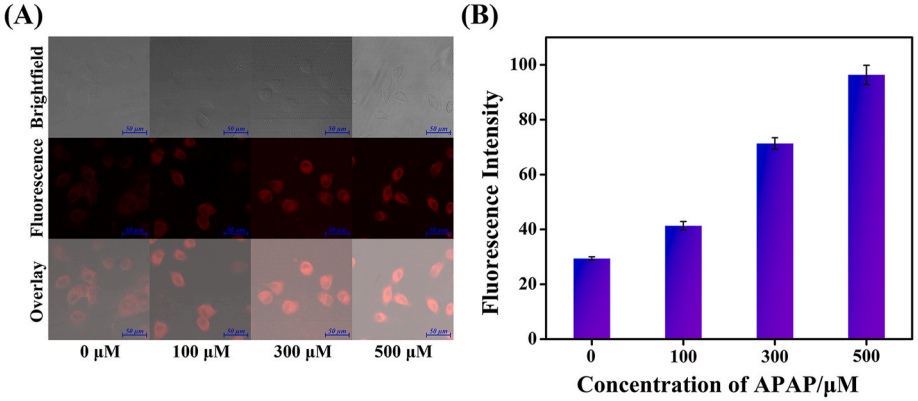

Fig. 8. (A) Fluorescence images in HepG2 cells successively treated with different concentrations of APAP (0, 100, 300, and 500 mM) and probe XH-2 (10 μM). (B) Bar graphs representing the corresponding fluorescence intensities of samples in (A).

concentration of APAP increased, which not only proves the generation of H_2O_2 induced by APAP in HepG2 cells, but also indicates the universality of probe XH-2. As all the above results manifested, probe XH-2 is suitable for use in visualizing the liver damage induced by APAP.

4. Conclusions

In conclusion, we reported a neoteric dual-signal colorimetric fluorescence probe for the detection of hydrogen peroxide. Probe XH-2 had high sensitivity and specificity owing to its specific recognition group. Based on its extremely low cytotoxicity, the probe was successfully applied to detect endogenous/exogenous hydrogen peroxide, to quantitatively determine the concentration level of hydrogen peroxide in HepG2 cells, and to visualize the liver injury induced by APAP. Collectively, based on these prominent performances, the probe XH-2 is a promising tool for evaluating and elucidating the diverse cellular functions of H_2O_2 in the living system to reveal the pathogenesis of many diseases.

Credit author contribution statement

Lanlan Xu: Conceptualization, Methodology, Software, Investigation, Validation, Data curation, Writing - original draft. Yu Zhang: Data analysis. Lihe Zhao: Data analysis. Hao Han: Data analysis. Siqi Zhang: Data analysis. Yibing Huang: Software, Validation. Xinghua Wang: Data curation. Daqian Song: Writing - review & editing. Pinyi Ma: Data curation, writing - review & editing. Ping Ren: Data curation, writing - review & editing.Ying Sun: Data curation.

Declaration of competing interest

The authors declare that they have no known competing financial interests or personal relationships that could have appeared to influence the work reported in this paper.

Acknowledgments

This work was supported by the National Natural Science Foundation of China (Grant Nos. 22004046 and 22074052), Science and Technology Developing Foundation of Jilin Province (Grant No. 20200602047ZP).

Appendix A. Supplementary data

Supplementary data to this article can be found online at https://doi.org/10.1016/j.talanta.2021.122578.

References

[1] V. Muhr, M. Buchner, T. Hirsch, D.J. Jovanović, S.D. Dolić, M.D. Dramićanin, O. S. Wolfbeis, Europium-doped GdVO4 nanocrystals as a luminescent probe for hydrogen peroxide and for enzymatic sensing of glucose, Sensor. Actuator. B Chem. 241 (2017) 349–356.
[2] M. Rahbari, S. Rahlfs, J.M. Przyborski, A.K. Schuh, N.H. Hunt, D.A. Fidock, G. E. Grau, K. Becker, Hydrogen peroxide dynamics in subcellular compartments of malaria parasites using genetically encoded redox probes, Sci. Rep. 7 (1) (2017) 10449.
[3] J.W. Liu, Y. Luo, Y.M. Wang, L.Y. Duan, J.H. Jiang, R.Q. Yu, Graphitic carbon nitride nanosheets-based ratiometric fluorescent probe for highly sensitive detection of H_2O_2 and glucose, ACS Appl. Mater. Interfaces 8 (49) (2016) 33439–33445.
[4] M. Ren, B. Deng, K. Zhou, X. Kong, J.Y. Wang, W. Lin, Single fluorescent probe for dual-imaging viscosity and H_2O_2 in mitochondria with different fluorescence signals in living cells, Anal. Chem. 89 (1) (2017) 552–555.
[5] Y. Chen, X. Shi, Z. Lu, X. Wang, Z. Wang, A fluorescent probe for hydrogen peroxide in vivo based on the modulation of intramolecular charge transfer, Anal. Chem. 89 (10) (2017) 5278–5284.
[6] T. Gong, J. Liu, Y. Wu, Y. Xiao, X. Wang, S. Yuan, Fluorescence enhancement of CdTe quantum dots by HBcAb-HRP for sensitive detection of H_2O_2 in human serum, Biosens. Bioelectron. 92 (2017) 16–20.
[7] H. Li, Q. Yao, J. Fan, J. Du, J. Wang, X. Peng, A two-photon NIR-to-NIR fluorescent probe for imaging hydrogen peroxide in living cells, Biosens. Bioelectron. 94 (2017) 536–543.
[8] H.H. Radeke, B. Meier, N. Topley, J. Floge, G.G. Habermehl, K. Resch, Interleukin 1-alpha and tumor necrosis factor-alpha induce oxygen radical production in mesangial cells, Kidney Int. 37 (2) (1990) 767–775.
[9] N. Houstis, E.D. Rosen, E.S. Lander, Reactive oxygen species have a causal role in multiple forms of insulin resistance, Nature 440 (7086) (2006) 944–948.
[10] A.G. Griesbeck, B. Öngel, M. Atar, New phthalimide-methionine dyad-based fluorescence probes for reactive oxygen species: singlet oxygen, hydrogen peroxide, and hypochlorite, J. Phys. Org. Chem. 30 (9) (2017), e3741.
[11] J. Xu, Y. Zhang, H. Yu, X. Gao, S. Shao, Mitochondria-targeted fluorescent probe for imaging hydrogen peroxide in living cells, Anal. Chem. 88 (2) (2016) 1455–1461.
[12] C. Feng, F. Wang, Y. Dang, Z. Xu, H. Yu, W. Zhang, A self-assembled ratiometric polymeric nanoprobe for highly selective fluorescence detection of hydrogen peroxide, Langmuir 33 (13) (2017) 3287–3295.
[13] X. Chen, X. Ren, L. Zhang, Z. Liu, Z. Hai, Mitochondria-targeted fluorescent and photoacoustic imaging of hydrogen peroxide in inflammation, Anal. Chem. 92 (20) (2020) 14244–14250.
[14] Y.J. Gong, D.D. Feng, W.N. Liu, J.K. Fang, S. Feng, A self-immolative near-infrared probe based on hemi-benzothiazolecyanine for visualizing hydrogen peroxide in living cells and mice, Dyes Pigments 186 (2021) 108954.
[15] H. Han, X. He, M. Wu, Y. Huang, L. Zhao, L. Xu, P. Ma, Y. Sun, D. Song, X. Wang, A novel colorimetric and near-infrared fluorescence probe for detecting and imaging exogenous and endogenous hydrogen peroxide in living cells, Talanta 217 (2020) 121000.
[16] P. Hou, S. Chen, G. Liang, H. Li, H. Zhang, Design of a facile fluorescent probe with a large Stokes shift for hydrogen peroxide imaging in vitro and in vivo, Spectrochim. Acta A 236 (2020) 118338.
[17] G. Jiang, C. Li, X. Liu, Q. Chen, X. Li, X. Gu, P. Zhang, Q. Lai, J. Wang, Lipid droplet-targetable fluorescence guided photodynamic therapy of cancer cells with an activatable AIE-active fluorescent probe for hydrogen peroxide, Adv. Opt. Mater. 8 (20) (2020) 2001119.
[18] D. Pham, U. Basu, I. Pohorilets, C.M. St Croix, S.C. Watkins, K. Koide, Fluorogenic probe using a mislow-evans rearrangement for real-Time imaging of hydrogen peroxide, Angew. Chem., Int. Ed. Engl. 59 (40) (2020) 17435–17441.
[19] R. Wang, Z. Bian, D. Zhan, Z. Wu, Q. Yao, G. Zhang, Boronic acid-based sensors for small-molecule reactive species: a review, Dyes Pigments 185 (2021), 108885-108885.
[20] W.X. Wang, W.L. Jiang, G.J. Mao, M. Tan, J. Fei, Y. Li, C.Y. Li, Monitoring the fluctuation of hydrogen peroxide in diabetes and its complications with a novel near-infrared fluorescent probe, Anal. Chem. 93 (6) (2021) 3301–3307.
[21] W.-X. Wang, W.-L. Jiang, Y. Liu, Y. Li, J. Zhang, C.-Y. Li, Near-infrared fluorescence probe with a large Stokes shift for visualizing hydrogen peroxide in ulcerative colitis mice, Sensor. Actuator. B Chem. (2020) 320.
[22] Y. Li, N. Duan, X. Wu, S. Yang, H. Tian, B. Sun, Novel fluorescent probe for the ratiometric detection of beta-galactosidase and its application in fruit, Food Chem. 328 (2020) 127112.
[23] W. Yao, Y. Cao, M. She, Y. Yan, J. Li, X. Leng, P. Liu, S. Zhang, J. Li, Imaging and monitoring the hydrogen peroxide level in heart failure by a fluorescent probe with a large Stokes Shift, ACS Sens. 6 (1) (2021) 54–62.
[24] H.C. Zhang, D.H. Tian, Y.L. Zheng, F. Dai, B. Zhou, Designing an ESIPT-based fluorescent probe for imaging of hydrogen peroxide during the ferroptosis process, Spectrochim. Acta A 248 (2021), 119264.
[25] R. Zhou, L. Niu, Y. Hu, Q. Qi, W. Huang, L. Yang, A novel dual-function fluorescent probe for the rapid detection of bisulfite and hydrogen peroxide in aqueous solution and living cells, Spectrochim. Acta A 248 (2021), 119226.
[26] M. Baccarin, B.C. Janegitz, R. Berte, F.C. Vicentini, C.E. Banks, O. Fatibello-Filho, V. Zucolotto, Direct electrochemistry of hemoglobin and biosensing for hydrogen peroxide using a film containing silver nanoparticles and poly(amidoamine) dendrimer, Mat. Sci. Eng. C-Mater. 58 (2016) 97–102.
[27] V. Carroll, B.W. Michel, J. Blecha, H. VanBrocklin, K. Keshari, D. Wilson, C. J. Chang, A boronate-caged [(1)(8)F]FLT probe for hydrogen peroxide detection using positron emission tomography, J. Am. Chem. Soc. 136 (42) (2014) 14742–14745.
[28] X. Qian Tang, Y. Dan Zhang, Z. Wei Jiang, D. Mei Wang, C. Zhi Huang, Y. Fang Li, Fe_3O_4 and metal-organic framework MIL-101(Fe) composites catalyze luminol chemiluminescence for sensitively sensing hydrogen peroxide and glucose, Talanta 179 (2018) 43–50.
[29] T. Matoba, H. Shimokawa, K. Morikawa, H. Kubota, I. Kunihiro, L. Urakami-Harasawa, Y. Mukai, Y. Hirakawa, T. Akaike, A. Takeshita, Electron spin resonance detection of hydrogen peroxide as an endothelium-derived hyperpolarizing factor in porcine coronary microvessels, Arterioscler, Thromb. Vasc. Biol. 23 (7) (2003) 1224–1230.
[30] H.M. Cocheme, C. Quin, S.J. McQuaker, F. Cabreiro, A. Logan, T.A. Prime, I. Abakumova, J.V. Patel, I.M. Fearnley, A.M. James, C.M. Porteous, R.A. Smith, S. Saeed, J.E. Carre, M. Singer, D. Gems, R.C. Hartley, L. Partridge, M.P. Murphy, Measurement of H_2O_2 within living Drosophila during aging using a ratiometric mass spectrometry probe targeted to the mitochondrial matrix, Cell Metabol. 13 (3) (2011) 340–350.
[31] Z. Zhou, Y. Li, W. Su, B. Gu, H. Xu, C. Wu, P. Yin, H. Li, Y. Zhang, A dual-signal colorimetric and near-infrared fluorescence probe for the detection of exogenous and endogenous hydrogen peroxide in living cells, Sensor. Actuator. B Chem. 280 (2019) 120–128.

[32] Z. Ma, Y. Sun, J. Xie, P. Li, Q. Lu, M. Liu, P. Yin, H. Li, Y. Zhang, S. Yao, Facile preparation of MnO_2 quantum dots with enhanced fluorescence via microenvironment engineering with the assistance of some reductive biomolecules, ACS Appl. Mater. Interfaces 12 (13) (2020) 15919–15927.
[33] J. Xie, D. Cheng, Z. Zhou, X. Pang, M. Liu, P. Yin, Y. Zhang, H. Li, X. Liu, S. Yao, Hydrogen peroxide sensing in body fluids and tumor cells via in situ produced redox couples on two-dimensional holey $CuCo_2O_4$ nanosheets, Mikrochim. Acta 187 (8) (2020) 469.
[34] J. Yao, T. Wu, Y. Sun, Z. Ma, M. Liu, Y. Zhang, S. Yao, A novel biomimetic nanoenzyme based on ferrocene derivative polymer NPs coated with polydopamine, Talanta 195 (2019) 265–271.
[35] L. Zhao, X. He, Y. Huang, J. Li, Y. Li, S. Tao, Y. Sun, X. Wang, P. Ma, D. Song, A novel ESIPT-ICT-based near-infrared fluorescent probe with large Stokes-shift for the highly sensitive, specific, and non-invasive in vivo detection of cysteine, Sensor. Actuator. B Chem. 296 (2019) 126571.
[36] L. Xu, M. Wu, L. Zhao, H. Han, S. Zhang, P. Ma, Y. Sun, X. Wang, D. Song, A novel highly sensitive and near-infrared fluorescent probe for detecting hypochlorite and its application in actual water sample and bioimaging, Talanta 215 (2020) 120892.